Supplement of The Cryosphere, 18, 3765–3785, 2024
https://doi.org/10.5194/tc-18-3765-2024-supplement

The Cryosphere Open Access EGU

Supplement of

Evaluating L-band InSAR snow water equivalent retrievals with repeat ground-penetrating radar and terrestrial lidar surveys in northern Colorado

Randall Bonnell et al.

Correspondence to: Randall Bonnell (randall.bonnell@colostate.edu)

Supplementary Tables

Table S1: Results from the test for atmospheric delays. Unwrapped phase (φ) was regressed against signal path length for snow-free pixels. The slope estimate (ß) and coefficient of determination (r^2) are reported for each date and polarization. RMSE was calculated with and without the estimated atmospheric corrections for four SNOTEL stations distributed throughout the UAVSAR flight line. Improvements in RMSE due to the atmospheric correction are reported as positive percents, while RMSE degradations are reported as negative percents.

	HH			HV			VH			VV		
InSAR Pair	**ß (φ /m)**	**r^2**	**RMSE Change (%)**	**ß (φ /m)**	**r^2**	**RMSE Change (%)**	**ß (φ /m)**	**r^2**	**RMSE Change (%)**	**ß (φ /m)**	**r^2**	**RMSE Change (%)**
12–19 February 2020	6.35e–5	0.14	-6.82	7.85e–5	0.22	-40.74	8.21e–5	0.21	-11.43	7.76e–5	0.29	No Data
19–26 February 2020	–3.23e–5	0.06	0.00	–3.08e–5	0.05	0.00	–2.58e–5	0.03	0.00	–2.97e–5	0.06	0.00
26 February – 12 March 2020	–9.24e–5	0.15	13.70	–1.82e–5	0.25	No Data	–1.34e–4	0.20	No Data	–3.17e–5	0.04	No Data
15–20 January 2021	–3.60e–5	0.08	-2.99	–4.76e–5	0.13	-9.80	–5.38e–5	0.16	-12.24	–3.99e–5	0.11	-2.44
20–27 January 2021	2.97e–5	0.04	12.50	4.45e–5	0.09	3.70	4.34e–5	0.07	15.79	2.65e–5	0.04	16.67
27 January – 3 February 2021	–1.20e–4	0.10	0.00	–1.16e–4	0.09	-3.23	–1.15e–4	0.08	-25.93	–1.01e–4	0.06	40.00
3–23 February 2021	–2.41e–4	0.58	No Data	No Data	No Data	No Data	–2.57e–4	0.63	No Data	No Data	No Data	No Data
23 February – 3 March 2021	5.69e–5	0.12	100.00	4.05e–5	0.06	12.50	6.56e–5	0.11	32.00	3.98e–5	0.07	-200.00
3–10 March 2021	–1.85e–4	0.54	-135.29	–1.72e–4	0.50	9.52	–1.84e–4	0.52	-312.50	–1.70e–4	0.53	-75.00
16–22 March 2021	–2.12e–4	0.22	-37.50	–2.64e–4	0.25	-140.00	–2.52e–4	0.28	-16.67	–2.40e–4	0.25	-300.00

Table S2: Weather Stations within the Rocky Mountains, Colorado UAVSAR flight line. Operators include the Colorado Avalanche Information Center (CAIC), Colorado State University (CSU), and the Natural Resources Conservation Service (NRCS). Locations are given as WGS84 latitude and longitude in decimal degrees (DD). Elevations are estimated from the Copernicus 30 m digital elevation model. Vegetation and canopy cover details obtained from the Copernicus Global Land Cover 100 m dataset (Buchhorn et al., 2020). Distances are measured from the station to the Michigan River field site.

Station Name	Abbreviation	Operator	Dates in Analysis	Location (DD)	Elevation (m)	Vegetation and Canopy Cover	Distance (km)
Cameron Pass Weather Station	CAIC	CAIC	1 Jan to 31 Mar 2020, 1 Jan to 15 Mar 2021	40.497, –105.9	3081	Evergreen >70%	2.5
Cameron Peak Field Site Weather Station	CPWS	CSU	14 Jan to 31 Mar 2021	40.564, –105.867	3012	Severely Burned 0%	5.4
Joe Wright SNOTEL	JW	NRCS	1 Dec to 30 Apr 2020, 1 Dec to 30 Apr 2021	40.533, –105.887	3100	Evergreen >70%	1.6
Lake Irene SNOTEL	LI	NRCS	1 Jan to 31 Mar 2020, 1 Jan to 31 Mar 2021	40.414, –105.820	3254	Evergreen 15–70%	13.1
Montgomery Snow Stake	MSS	CSU	1 Jan to 31 Mar 2021	40.544, –105.881	3067	Evergreen >70%	2.9
Phantom Valley SNOTEL	PV	NRCS	1 Jan to 31 Mar 2020, 1 Jan to 31 Mar 2021	40.398, –105.846	2758	Herbaceous 0%	13.9
Willow Park SNOTEL	WP	NRCS	1 Jan to 31 Mar 2020, 1 Jan to 31 Mar 2021	40.434, –105.736	3263	Evergreen 15–70%	16.2

Table S3: Field site SWE change (ΔSWE) values for the interval board, GPR, and UAVSAR at co-located GPR pixels for the UAVSAR time series presented in the manuscript (all date intervals used HH polarization, except the VH polarization used for 3–23 February 2021). The interval board reports the mean because only two interval boards were deployed during the surveys.

Date Interval	Interval Board Mean ΔSWE (mm)	GPR Median ΔSWE (mm)	UAVSAR Median ΔSWE (mm)
12–19 February 2020	43	98	97
19–26 February 2020	31	15	16
26 February – 12 March 2020	21	10	8
15–20 January 2021	22.5	13	14
20–27 January 2021	27	30	28
27 January – 3 February 2021	4	0	–2
3–23 February 2021	73	112	112
23 February – 3 March 2021	14	17	16
3–10 March 2021	4	1	4
16–22 March 2021	14	30	34

Table S4: Evaluation of the four polarizations (HH, HV, VH, and VV) of UAVSAR ΔSWE retrievals using GPR ΔSWE retrievals. For each polarization, the number of observations (n), the root mean squared error (RMSE), and Pearson's correlation coefficient (r) are given. Instances where no data was available are indicated by hyphens. Although the manuscript presents the HH polarization results, the overall HH statistics presented here differ from the overall statistics presented in the manuscript because the manuscript includes the 3–23 February 2021 VH pair in the presented time series.

	HH			HV			VH			VV		
InSAR Pair	**n**	**RMSE (mm)**	**r**	**n**	**RMSE (mm)**	**r**	**n**	**RMSE (mm)**	**r**	**n**	**RMSE (mm)**	**r**
12–19 February 2020	110	34	–0.03	122	32	–0.02	130	32	–0.03	-	-	-
19–26 February 2020	143	29	0.13	143	30	0.11	143	28	0.09	143	28	0.19
26 February – 12 March 2020	130	26	0.13	117	28	0.15	118	27	0.08	129	26	0.02
15–20 January 2021	390	19	0.13	401	20	0.16	379	20	0.18	400	17	0.08
20–27 January 2021	337	16	0.19	319	15	0.15	334	16	0.10	382	17	0.25
27 January – 3 February 2021	373	16	0.07	362	15	0.18	350	15	0.19	379	16	0.05
3–23 February 2021	-	-	-	-	-	-	185	33	0.01	-	-	-
23 February – 3 March 2021	396	19	0.20	402	20	0.15	398	20	0.16	390	19	0.17
3–10 March 2021	362	23	–0.24	364	21	–0.15	357	21	–0.16	376	19	–0.18
16–22 March 2021	407	22	0.07	410	20	0.09	429	20	0.13	426	21	0.05
Overall	2648	21	0.66	2640	21	0.68	2823	22	0.80	2625	19	0.48

Supplementary Figures

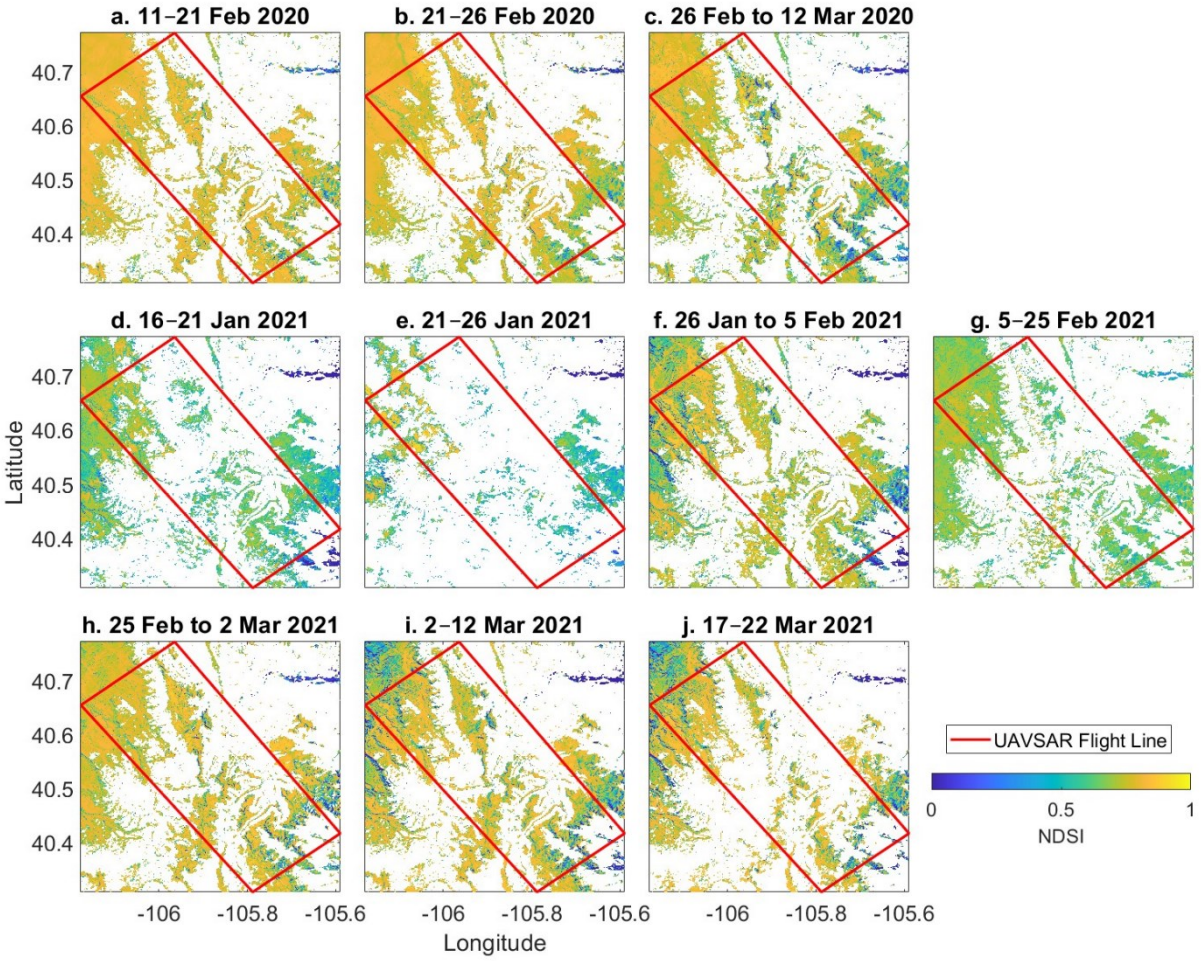

Figure S1: NDSI (Equation A3) maps for each UAVSAR flight interval calculated from composited Sentinel-2 Level 2A imagery. Clouds and forests (Buchhorn et al., 2020) were removed from this analysis. Snow-free pixels were identified as NDSI <0.20.

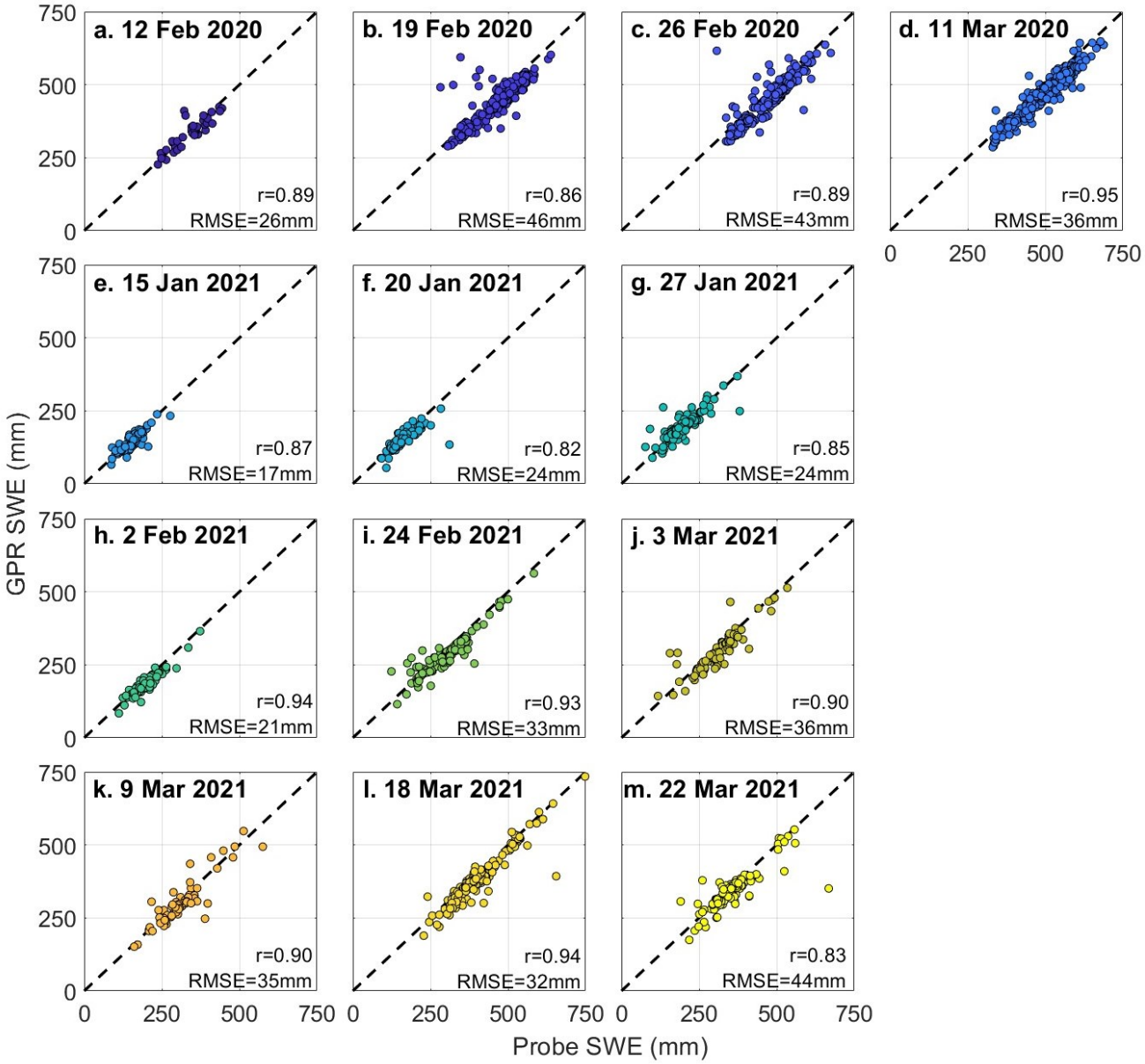

Figure S2: Comparison between GPR SWE retrievals and SWE converted from probed depths for each survey date. Median GPR SWE was calculated within a 1.5 m radius for each probed point. The number of GPR points used for estimating the median GPR SWE for comparison with probed SWE varied, but exceeded 10 points per probe in most cases. Points are colored by date. In 2020, ~200 probed points were collected per survey date, whereas ~120 were collected per survey date in 2021. Overall Pearson's correlation coefficient = 0.97 and RMSE = 35 mm.

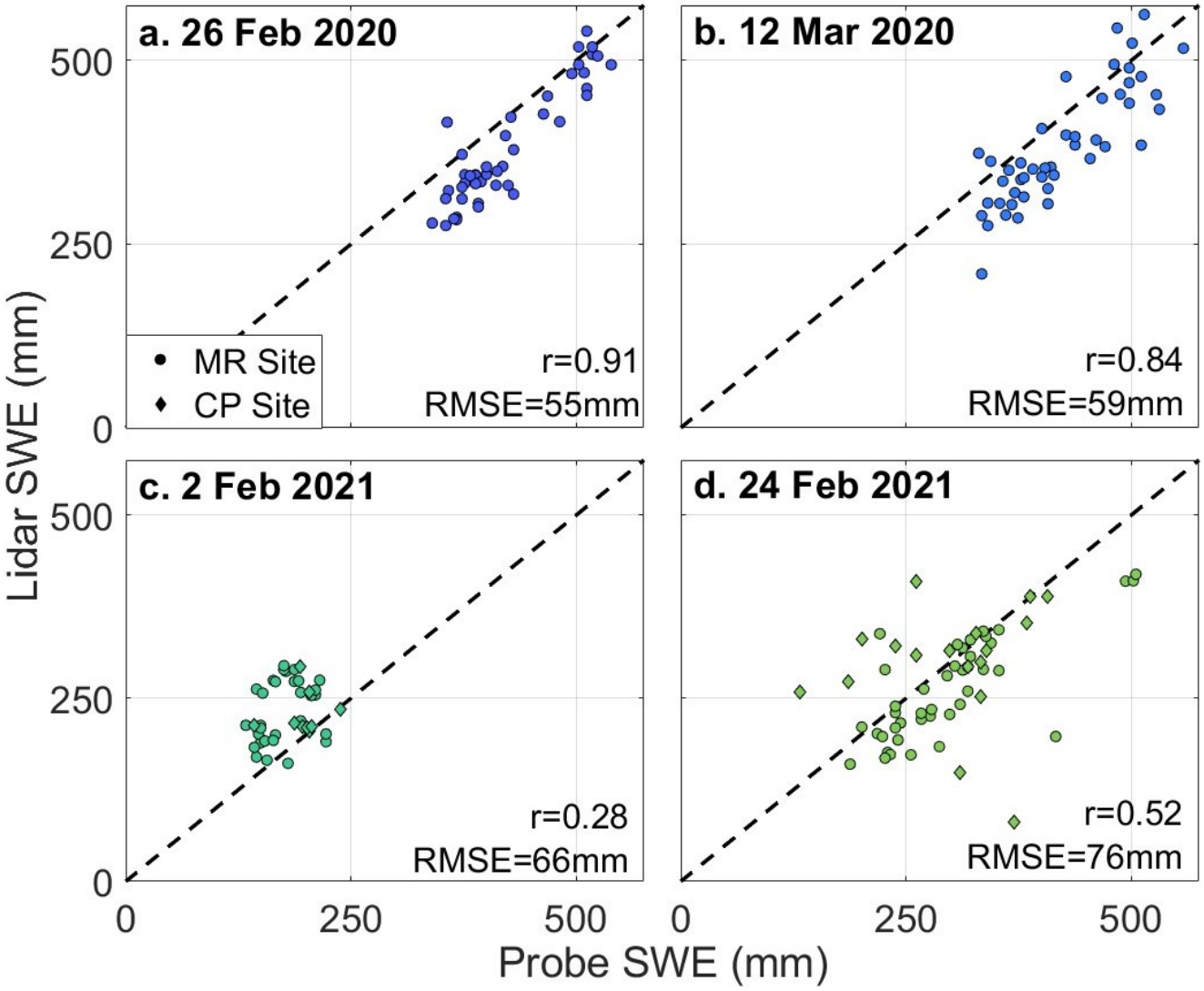

Figure S3: Comparisons between TLS SWE retrievals and SWE converted from probed depths for each lidar survey date. Probed SWE points represent the average of the one to two probed points within a single TLS pixel. The TLS surveys conducted on 10 February 2021 were adjusted to 2 February 2021 by using SWE measured on the interval boards on 10 February 2021. Overall Pearson's correlation coefficient = 0.83 and RMSE = 66 mm. Points are colored by date.

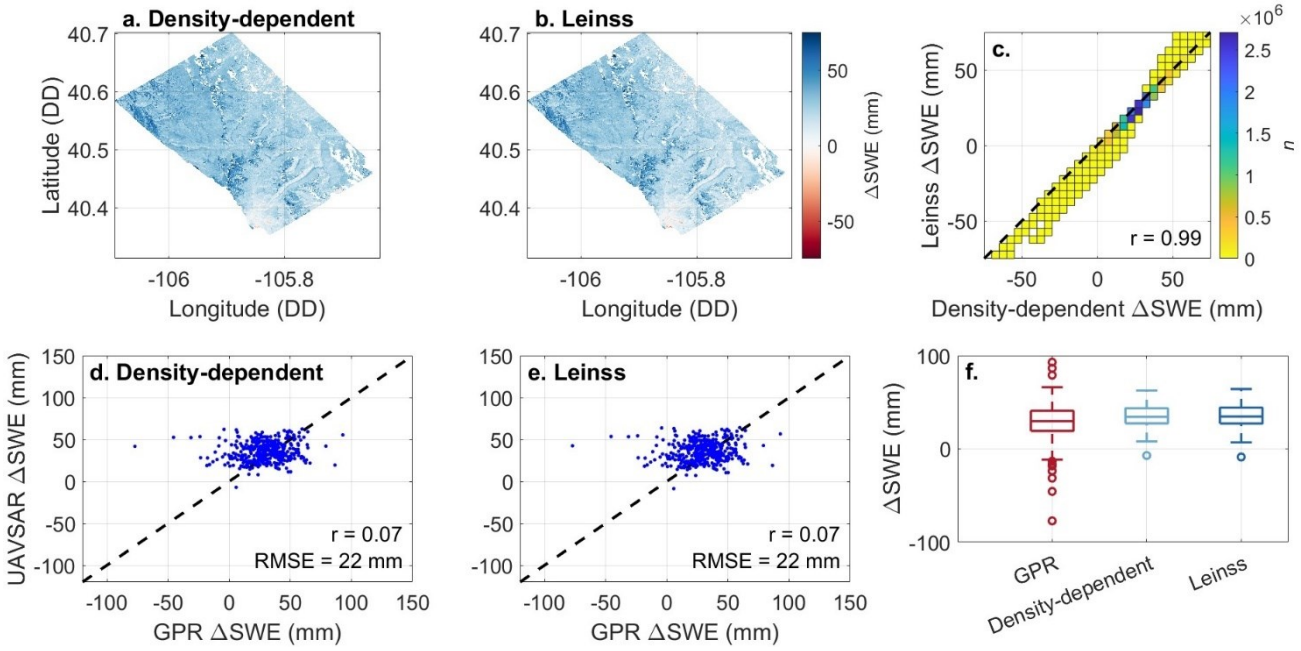

Figure S4: Evaluation of the Leinss et al. (2015) approximation for ΔSWE retrievals from the 16–22 March 2021 HH InSAR pair. ΔSWE retrievals calculated from (a) the density-dependent equation used in the manuscript and (b) the Leinss et al. (2015) approximation. (c) Comparison between the density-dependent and Leinss et al. (2015) approximation ΔSWE retrievals. Comparison of GPR ΔSWE retrievals with (d) the density-dependent method and (e) the Leinss et al. (2015) approximation. (f) Box plot distributions of ΔSWE retrievals from the three methods. For plots a–c, the range of ΔSWE is limited to ±75 mm, which represents >99% of the distribution.

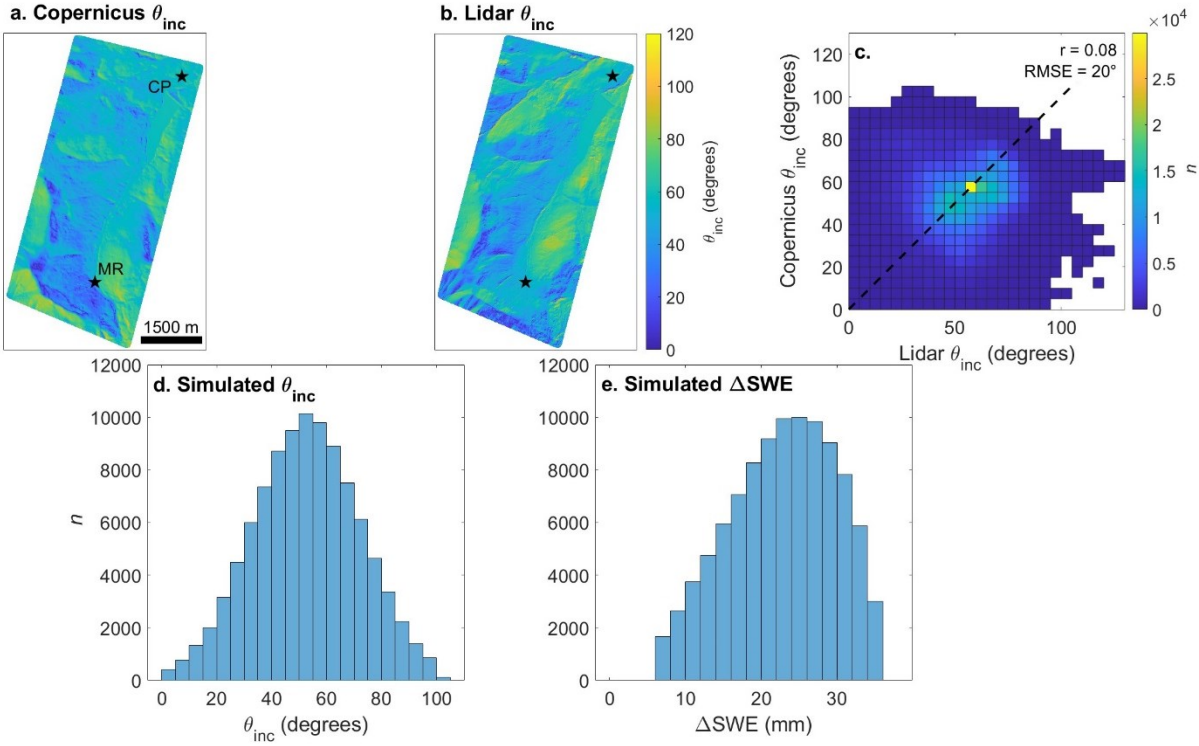

Figure S5: Evaluation of the Copernicus-derived incidence angles. Incidence angles derived from (a) the Copernicus 30 m DEM and (b) the lidar 0.5 m DEM (Adebisi et al., 2022). (c) Two-dimensional histogram showing the comparison between the two sets of incidence angles. Distributions from the Monte Carlo simulation of (d) incidence angles and (e) the corresponding ΔSWE retrievals.

Data Availability

GPR datasets and the lidar 0.5 m DEM are archived with the NSIDC (Adebisi et al., 2022; Bonnell et al., 2022; McGrath et al., 2021). Probed snow depths from both seasons are under review at the NSIDC. SNOTEL station data is publicly available from the NRCS and was used for the following stations: Joe Wright (https://wcc.sc.egov.usda.gov/nwcc/site?sitenum=551), Lake Irene (https://wcc.sc.egov.usda.gov/nwcc/site?sitenum=565), Willow Park (https://wcc.sc.egov.usda.gov/nwcc/site?sitenum=870), and Phantom Valley (https://wcc.sc.egov.usda.gov/nwcc/site?sitenum=688). TLS point clouds are available at UNAVCO Inc. (Williams, 2021). NASA UAVSAR datasets are available from UAVSAR or the ASF DAAC, including InSAR pair products (i.e., unwrapped phase, coherence) and SLC products (i.e., look vectors; NASA UAVSAR, 2020; NASA UAVSAR, 2021). The Copernicus 30 m DEM, Copernicus Global 100 m Land Cover Dataset, and Sentinel-2 Level 2A imagery were accessed via Google Earth Engine (Gorelick et al., 2017).

References

Adebisi, N., Marshall, H., O'Neel, S., Vuyovich, C. M., Hiemstra, C., and Elder, K.: SnowEx20-21 QSI Lidar DEM 0.5m UTM Grid, Version 1 [Data Set], https://doi.org/10.5067/YO583L7ZOLOO, 2022.

Bonnell, R., McGrath, D., Zeller, L., Bump, E., and Olsen-Mikitowicz, A.: SnowEx21 Cameron Pass Ground Penetrating Radar, Version 1, National Snow and Ice Data Center Distributed Active Archive Center [Data Set], https://doi.org/10.5067/SRWGLYCB6ZC4, 2022.

Buchhorn, M., Smets, B., Bertels, L., Roo, B. D., Lesiv, M., Tsendbazar, N.-E., Herold, M., and Fritz, S.: Copernicus Global Land Service: Land Cover 100m: collection 3: epoch 2019: Globe (Version V3.0.1), Zenodo [data set], https://doi.org/10.5281/zenodo.393050, 2020.

European Space Agency: Copernicus Global Digital Elevation Model, Distributed by Google Earth Engine [data set], https://doi.org/10.5270/ESA-c5d3d65, 2021.

European Space Agency: Copernicus Sentinel data, Distributed by Google Earth Engine [data set], https://doi.or/10.5270/S2_-6eb6imz, 2022.

Kampf, S., Sears, M., Miller, Q., Puntenney-Desmond, K., Barnard, D., Green, T., Erskine, R., Sitterson, J., Kiewiet, L., Reis, W., and McGrath, D.: Cameron Peak Fire stream and weather data WY2021, HydroShare [data Set], http://www.hydroshare.org/resource/a15f503ab00b4980a4bfbe7e8552f9a3, 2022.

Leinss, S., Wiesmann, A., Lemmetyinen, J., and Hajnsek, I.: Snow water equivalent of dry snow measured by differential interferometry, IEEE Journal of Selected Topics in Applied Earth Observations and Remote Sening, 8, 3773-3790, https://doi.org/10.1109/JSTARS.2015.2432031, 2015.

McGrath, D., Bonnell, R., Olsen-Mikitowicz, A., Duncan, C., and Grabowski, J.: SnowEx20 Cameron Pass Ground Penetrating Radar, Version 1, NASA National Snow and Ice Data Center Distributed Active Archive Center [data set], https://doi.org/10.5067/U4Q3X27BMRR4, 2021.

NASA UAVSAR: Rocky Mountains, Colorado Flight Line, Alaska Satellite Facility Distributed Active Archive Center [data set], 2020.

NASA UAVSAR: Rocky Mountains, Colorado Flight Line, Alaska Satellite Facility Distributed Active Archive Center [data set], 2021.

Williams, K.: Cameron Pass NASA SnowEx, UNAVCO Inc. [data set], https://tls.unavco.org/projects/U-077/, 2021.